Letter

Breakdown of sound in superfluid helium

Marc D. Nichitiu,[1] Craig Brown,[2] and Igor A. Zaliznyak[1,*]

[1]*Condensed Matter Physics and Materials Science Division, Brookhaven National Laboratory, Upton, New York 11973, USA*

[2]*NIST Center for Neutron Research, National Institute of Standards and Technology, Gaithersburg, Maryland 20899, USA*

(Received 15 September 2023; accepted 23 January 2024; published 13 February 2024)

As elementary particles carry energy and momentum in the Universe, quasiparticles are the elementary carriers of energy and momentum quanta in condensed matter. And, as elementary particles, under certain conditions quasiparticles can be unstable and decay, emitting pairs of less energetic ones. Pitaevskii [Sov. Phys. JETP **9**, 830 (1959)] proposed that such processes exist in superfluid helium, a quantum fluid where the very concept of quasiparticles was borne by Landau and which presented the first notable success of that concept. Pitaevskii's decays have important consequences, including the possible breakdown of a quasiparticle [M. B. Stone *et al.*, Nature (London) **440**, 187 (2006)]. Here, we present neutron scattering experiments, which provide evidence that such decays explain the collapsing lifetime (strong damping) of higher-energy phonon-roton sound-wave quasiparticles in superfluid helium. This damping develops when helium is pressurized towards crystallization, or warmed towards approaching the superfluid transition. Our results resolve a number of puzzles raised by previous experiments and reveal the ubiquity of quasiparticle decays and their importance for understanding quantum matter.

DOI: 10.1103/PhysRevB.109.L060502

The quasiparticle concept is a cornerstone of our understanding of many-body atomic systems that make up materials around us. Heat, sound, electric current, and their interconversion in materials which underpin a broad range of technologies, can all be understood as being carried by elementary excitations, the quasiparticles. These elementary excitations were devised by Landau to describe the properties of superfluid helium isotope ^{4}He, a quantum liquid with zero viscosity which can flow without any friction [1], and led to a triumph in our understanding of quantum condensed matter [2–5]. By postulating the energy-momentum relation $\epsilon(Q)$ of phonon-roton quasiparticles—sound waves carrying energy and momentum in superfluid ^{4}He—Landau very accurately explained essentially all of its experimentally observed properties ($Q = p/\hbar$ is the wave vector of the corresponding wave with wavelength $\lambda = 2\pi/Q$, p is momentum, and $\hbar$ is Planck's constant). For quasiparticles, this $\epsilon(Q)$ dispersion replaces Einstein's famous relation, $\epsilon(p) = \sqrt{(pc)^2 + (mc^2)^2}$ (c is the velocity of light and m is the particle mass at rest), or its nonrelativistic Newtonian version, $\epsilon(p) = p^2/2m$, which describe elementary particles.

A detailed theory of viscosity behavior in superfluid helium was subsequently developed by Landau and Khalatnikov (LK) based upon the idea that transport phenomena can be described in terms of collisions between the quasiparticles, which form a nearly ideal gas [5,6]. The resulting phonon-roton transport theory provided very good agreement with the experimental values of the viscosity coefficient at low temperatures. A notable deviation observed in a temperature region near the superfluid transition [the λ point, $T_\lambda \approx 2.19$ K at atmospheric pressure $\approx$1 bar, Fig. 1(a)] was ascribed to the failure of the approximation where phonon and roton quasiparticles are treated as nearly ideal gases. Here, we show that it is the quasiparticle breakdown processes that are at the origin of the observed deviation.

That Landau's guess for $\epsilon(Q)$ turned out to be remarkably accurate was confirmed by inelastic neutron scattering (INS), a technique that allows to directly detect quasiparticles [7–22]. By measuring the probability for a neutron passing through a superfluid helium (or another material) to scatter losing some of its energy and momentum, one can experimentally determine the energy-momentum relationship of the quasiparticles that are created as a result. Recent progress in neutron scattering technology allows to conduct such measurements with exceptional precision [19,20]. It was shown [20] that using the precise INS measurements of quasiparticle dispersion in superfluid ^{4}He as an input to Landau theory provides an exceptionally accurate description of specific heat and other thermodynamic properties at low temperatures, while notable discrepancies are present within about 0.5 K below the superfluid transition. By exploring in detail the behavior of phonon-roton quasiparticle in this region in our INS experiments (Fig. 1), we show that the observed failure of the theoretical description is rooted not in the nonideal nature of the phonon and roton gases implied by the most simple version of the Landau theory used in Ref. [20], but, in fact, in the failure of the quasiparticle description at its core borne by the quasiparticle decay processes.

Color contour plots in Figs. 2(a)–2(e) show a spectral density of INS intensity obtained in our measurements at different pressures and at low temperatures within the superfluid phase (Fig. 1; see Fig. S1 in the Supplemental Material for the measured neutron intensity [23]). The intense curvy line traces the

*zaliznyak@bnl.gov

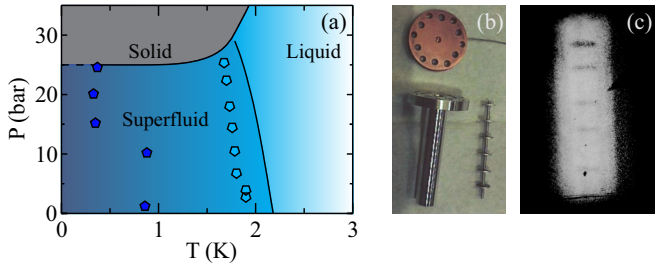

FIG. 1. The (P, T) phase diagram of superfluid ^{4}He with locations of our INS measurements. (a) Lines indicate superfluid, normal liquid, and solid phase boundaries; dark-solid upward-pointing pentagons represent the low-temperature measurements with incident neutron energy $E_i = 3.55$ meV shown in Fig. 2, and light-solid downward pentagons represent measurements closer to the superfluid-to-normal-liquid transition with $E_i = 3.27$ meV shown in Fig. 3. (b) The Al sample cell (0.95 cm inner, 1.25 cm outer diameter) used in our measurements, with an Al rod with ≈1 cm spaced Cd dividers and a copper top flange with a ≈0.15 cm diameter input capillary. (c) Transmission neutron radiograph of the (empty) assembled sample cell, with shades from neutron-absorbing Cd dividers visible. The resulting small, ≈0.7 cm^3, scattering volume of each subcell markedly reduces the parasitic double scattering effects compared to previously reported measurements [14,15,17,20,22].

phonon-roton quasiparticle dispersion (the linear rise at small Q is the phonon part, while the minimum near $Q \approx 1.9$ Å^{-1}, following Landau, is called the roton). The narrow peak of the measured scattering intensity in Figs. 2(f)–2(l), which reveals the quasiparticle, has a width which is approximately consistent with the experimental energy resolution of our measurement (see also Supplemental Material [23] and the discussion below). Zero, or a small, intrinsic energy width of the INS peak indicates an infinite, or very long, quasiparticle lifetime. Ideally, quasiparticles with an infinite lifetime τ describe stationary excited states of the system that are the eigenstates of energy and momentum with the eigenvalues in a one-to-one correspondence forming unique pairs (ϵ, Q), which determine the quasiparticle dispersion $\epsilon(Q)$. INS measures the probability of different energy-momentum excited states of the system and in such an ideal case, $\tau = \infty$, the probability distribution is Dirac's delta function, $\delta(\epsilon - \epsilon(Q))$, of zero width, $\Gamma = \hbar/\tau = 0$ (in practice, in an INS experiment the measured distribution is broadened by a finite instrument resolution resulting from a less than perfect discrimination between different energies and wave vectors). In such a case, the knowledge of the quasiparticle dispersion $\epsilon(Q)$ is sufficient to construct the systems's partition function and accurately describe all of its thermal properties, which explains the power of the quasiparticle concept.

While considering quasiparticle collisions and applying Boltzmann transport theory allows us to obtain a quantitative description of transport phenomena in superfluid helium, such as convection and viscosity [5,6], collisions also shorten the quasiparticle lifetime. As for elementary particles, collisions can change the quasiparticles' (ϵ, Q) identities, which means that in the presence of other excited states, each elementary excitation acquires a finite lifetime. The more quasiparticles are excited with increasing temperature, storing the system's thermal energy, the shorter their lifetime becomes due to collisions, which increase in frequency. Landau and Khalatnikov (LK) obtained an accurate description of these effects, where the roton peak width is proportional to the number of thermally excited rotons, $\Gamma \sim \sqrt{T} e^{-\frac{\Delta(T)}{k_B T}}$ [Δ is the minimum energy of the roton (Fig. 2) which depends on P and T]. This was checked in a number of INS experiments and was shown to work well up to ≈1.5 K [24–26]. Apparent deviations from the LK behavior of Γ at higher temperatures were considered to reflect the inadequacy of the experimental model in extracting quasiparticle parameters rather than any inherent inaccuracy of the LK model [17].

At zero temperature, there are no collisions that would limit the quasiparticle lifetime because there are no thermally excited quasiparticles. Hence, according to LK, $\Gamma(T) = 0$ at $T = 0$, which means that the measured width of the INS spectrum should be resolution limited. However, quasiparticles, as some elementary particles, can be unstable with respect to decays if these are allowed by quantum-mechanical conservation laws. Such spontaneous decays can lead not only to a finite lifetime, but also to a complete disappearance of the quasiparticle states. Landau conjectured that the quasiparticle spectrum in superfluid ^{4}He could terminate at large Q where its energy increases such that decays into roton pairs become kinematically allowed, i.e., the quasiparticle dispersion enters the energy range of the continuum of two-roton states, $\epsilon(Q) \geqslant 2\Delta$. An elegant theory of this phenomenon was developed by Pitaevskii to whom the problem was posed [27,28]. Not only did this theory predict the spectrum end point Q_c, but it also explained the downward bending of the dispersion on approaching the Q_c, a puzzling behavior observed in experiment [8–21,29]. While similar effects of spontaneous quasiparticle decays have been also observed by INS in quantum magnets [30,31], revealing these to be a ubiquitous property of quantum matter, the unambiguous experimental identification of Q_c in superfluid helium still remains a challenge [19,20].

While the spectrum termination point at high Q is outside the range of our present measurements, the effects of decay interactions transpire in our data at higher pressures (Fig. 2). As the roton gap $\Delta(P)$ decreases with the pressure increasing towards crystallization (which for $T \approx 0$ occurs at $P \approx 25$ bars, Fig. 1) [9,10], the threshold for the onset of two-roton states also decreases. When this threshold $2\Delta(P)$ approaches the local dispersion maximum near $Q_m \approx 1.2$ Å^{-1} (quasiparticles in this range are conventionally called a "maxon"), the interaction effects first lead to "squaring" of the dispersion, which becomes increasingly clear for $P \geqslant 15$ bars. This energy-level-repulsion effect between the quasiparticle and the two-roton continuum, similar to that predicted by Pitaevskii, is prominently displayed by the increasing (with pressure) discrepancy between the measured $\epsilon(Q)$ and the fitted Bogolyubov dispersion for noninteracting quasiparticles [32–37], which accurately describes the lower-energy region of the phonon-roton dispersion where the effects of interaction are small (dashed curve in Fig. 2; see also Figs. S1 and S5 [23]).

At the highest pressure of our measurements, $P =$ 24.6 bars, the maxon intensity notably decreases and an

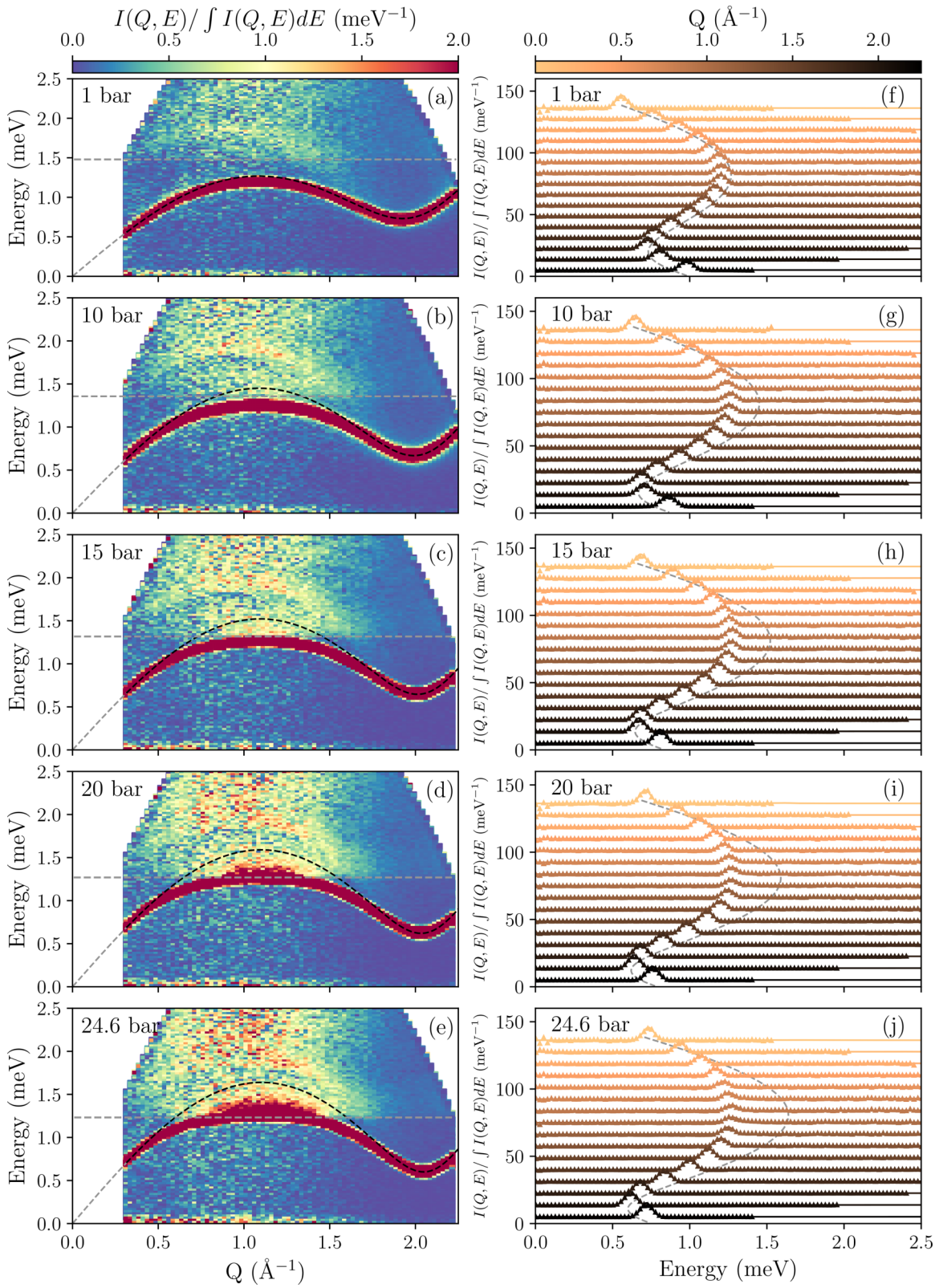

FIG. 2. Phonon-roton quasiparticle in superfluid ^{4}He. [(a)–(e)] Color contour maps of the spectral density of the measured neutron scattering intensity at different pressures, $P = 1.22(3)$, 10.19(3), 15.20(3), 20.11(2), and 24.57(4) bars (top to bottom), tracking the quasiparticle dispersion $\epsilon(Q)$. The dashed curve is the fitted Bogolyubov dispersion [32–37] without accounting for multiparticle interactions (see Supplemental Material [23] for the details of dispersion fitting), and the horizontal dashed line marks the decay threshold energy 2Δ. [(f)–(j)] Selected constant-Q cuts of the corresponding spectral density of the measured neutron intensity with fits to the resolution-corrected damped harmonic oscillator (DHO) line shape. The width of the peak is consistent with the instrument resolution ($\Delta E_{\text{res}} \approx 0.1$ meV), with a visible deviation at the highest pressures near the top of dispersion, where pair decays become active.

indication of finite lifetime (finite peak width) appears near Q_m, extending similar observation of Ref. [20]. With the further decrease of the two-roton threshold energy at higher pressure, the quasiparticle spectrum can be expected to terminate at two wave vectors, Q_{c1} and Q_{c2} around Q_m, opening an entire region of excited states in the $[Q_{c1}, Q_{c2}]$ range to higher-energy excitations. Strikingly, this does not happen. Instead, with a tiny increase in pressure to $\approx$25 bars, superfluid ^{4}He solidifies in a first-order phase transition. This occurs well before the roton energy softens to zero, as could be expected for a soft-mode second-order transition. Hence, it appears as if the (avoided) quasiparticle breakdown is actually the cause of the observed "premature" crystallization, a well-known puzzling behavior of the superfluid ^{4}He. Interestingly, this observation can be understood from a simple quantum-mechanical argument. Superfluid ^{4}He at ambient pressure remaining liquid down to an absolute zero temperature hinges on a fine balance between the energy of zero-point quantum motion of the liquid and the solid phases. In a superfluid, zero-point energy is determined by the quasiparticle dispersion, $E_0 = \sum_Q \frac{1}{2}\epsilon(Q)$. When the quasiparticles break down between Q_{c1} and Q_{c2}, higher-energy excitations contribute to zero-point motion and its energy increases to become larger than that of a solid, causing crystallization.

With temperature increasing towards the λ point, the roton energy and the two-roton threshold further decrease [9,16,17]. For temperatures $\sim 0.8T_\lambda$ of our INS measurements presented in Fig. 3 (1.7–1.9 K, Fig. 1), even at a low pressure of 2.75 bars the two-roton threshold intercepts the phonon-roton dispersion, allowing decay processes within a finite Q-range around Q_m [Fig. 3(a)]. While the entire quasiparticle spectrum already has a substantial thermal width, $\lesssim$0.5 meV, because of the finite LK lifetime due to collisions at these temperatures [9,17] (see also Fig. 4), there is a marked additional blurring near the top of the dispersion due to decays. This effect is most clearly seen at low Q, where for energies below the two-roton threshold [horizontal dashed line in Figs. 3(a)–3(e)], the phonon quasiparticle in the linear part of the dispersion presents a well-defined peak in the measured INS intensity at each $Q < Q_{c1}$, only broadened by a finite lifetime [bright streak at low Q in Figs. 3(a)–3(e)]. The peak broadens dramatically for energies above the threshold, $\epsilon > 2\Delta$, revealing the effect of decays. The same is the situation in the roton region, where an LK collision-lifetime-broadened quasiparticle exists below the 2Δ threshold, for $Q > Q_{c2}$. We note that at finite-temperature quasiparticle breakdown for $Q \in [Q_{c1}, Q_{c2}]$ does not lead to crystallization because the liquid state is entropically stabilized. Albeit access to higher-energy excited states does increase the system's internal energy E, it also adds to the entropy S whose contribution at finite T lowers the free energy of the system, $E - k_B T \ln S$.

Comparing Figs. 3(a)–3(e), we observe that the decay region expands as pressure increases towards crystallization, blurring an increasingly wider part of the quasiparticle dispersion around Q_m. In this ever-increasing Q range, the quasiparticle instability to decays invalidates the LK-type theoretical approach to describing transport and thermal phenomena in superfluid ^{4}He in terms of quasiparticles and their collisions. This observation explains a previously reported discrepancy, growing at higher temperatures and pressures, between the LK theory and INS experiment [9,10,16,17].

In the presence of a finite lifetime, the quasiparticle spectral function measured by INS transforms from a Dirac delta function for $\tau = \infty$ to that of a damped harmonic oscillator (DHO), $I(\epsilon, Q) \sim \frac{2\Gamma\epsilon}{[\epsilon^2-(\epsilon^2(Q)+\Gamma^2)]2+(2\Gamma\epsilon)^2}$. For the underdamped case, this expression is equivalent to the difference of two Lorentzian functions centered at $\pm\epsilon(Q)$ and with full width at half maximum (FWHM), $2\Gamma = 2\hbar/\tau$ [38]; at finite T, it is also weighted by the detailed balance factor [17,37]. We therefore quantify the effects of quasiparticle spectrum broadening by fitting the measured INS intensity at each Q to the DHO response with the quasiparticle energy $\epsilon(Q)$, intensity $I(Q)$, and Q-dependent width $\Gamma(Q)$ as parameters. The corresponding fits are shown by solid lines in Figs. 2(f)–2(j) and 3(f)–3(j) and the obtained width $\Gamma(Q)$ is presented in Fig. 4.

For the low-temperature data of Fig. 2, there is a small but discernible width, $\sim$0.01 meV, for the 1-bar and 10-bars data measured at $T \approx 0.9$ K, which is larger than the LK collisional broadening and probably indicates decays into phonon pairs such as discussed in Ref. [20] [Figs. 4(a) and 4(b)]. For the 15- and 20-bars, ≈ 0.35 K data, there is no discernible broadening, consistent with LK and with the pressure-induced stability of the phonon spectrum [20] (except for a small effect near Q_m at 20 bars, indicative of the onset of decays into roton pairs). At 24.6 bars, also measured at $\approx$0.35 K, fitting reveals a noticeable width, $\Gamma > 0.02$ meV, exceeding that seen at 0.9 K, for wave vectors near Q_m, clearly indicating the effect of quasiparticle decays, which can also be identified in Fig. 2(e) and Fig. S1(j) [23]. The symbols with a fitted parabolic dashed line in Fig. 4(a) show the pressure-dependent momentum region where decays are allowed for noninteracting quasiparticles with the fitted Bogolyubov dispersion [23,32–37] shown in Figs. 2(a)–2(e). In reality, the interaction-induced decrease of dispersion maximum pushes this region to higher pressures, $\gtrsim$20 bars.

The decay region explodes at higher temperatures, as the roton energy decreases [Fig. 4(c)]. The two-roton decays add substantially, up to $\gtrsim$100% for the temperatures 1.7–1.9 K we measured, to the LK collisional thermal damping, which, albeit already large, only dominates at low energies, $E \lesssim 2\Delta$ [Fig. 4(d)]. It is therefore not surprising that a quasiparticle transport theory, which only accounts for collisions and neglects decays, could diverge from experiment at temperatures near the superfluid transition and at pressures close to crystallization where the roton gap becomes small and the decay region is large. While extracting the absolute values of Γ at higher temperatures is tedious and can be model dependent, as discussed in detail by Glyde [21], the wave-vector dependence $\Gamma(Q)$ established in our measurement is clear and unambiguous in revealing the decay region $[Q_{c1}, Q_{c2}]$, whose dependence on pressure is governed by the phonon-roton dispersion (Fig. 4).

Superfluid helium presents the standard model of quasiparticle physics in quantum matter [5,28,32]. An understanding and accurate description of the quasiparticles in helium has been foundational for the development of theories of many-body quantum states and is fundamental for the progress in our ability to describe and control quantum systems of Bose particles, from trapped atoms to quantum magnets [30,31].

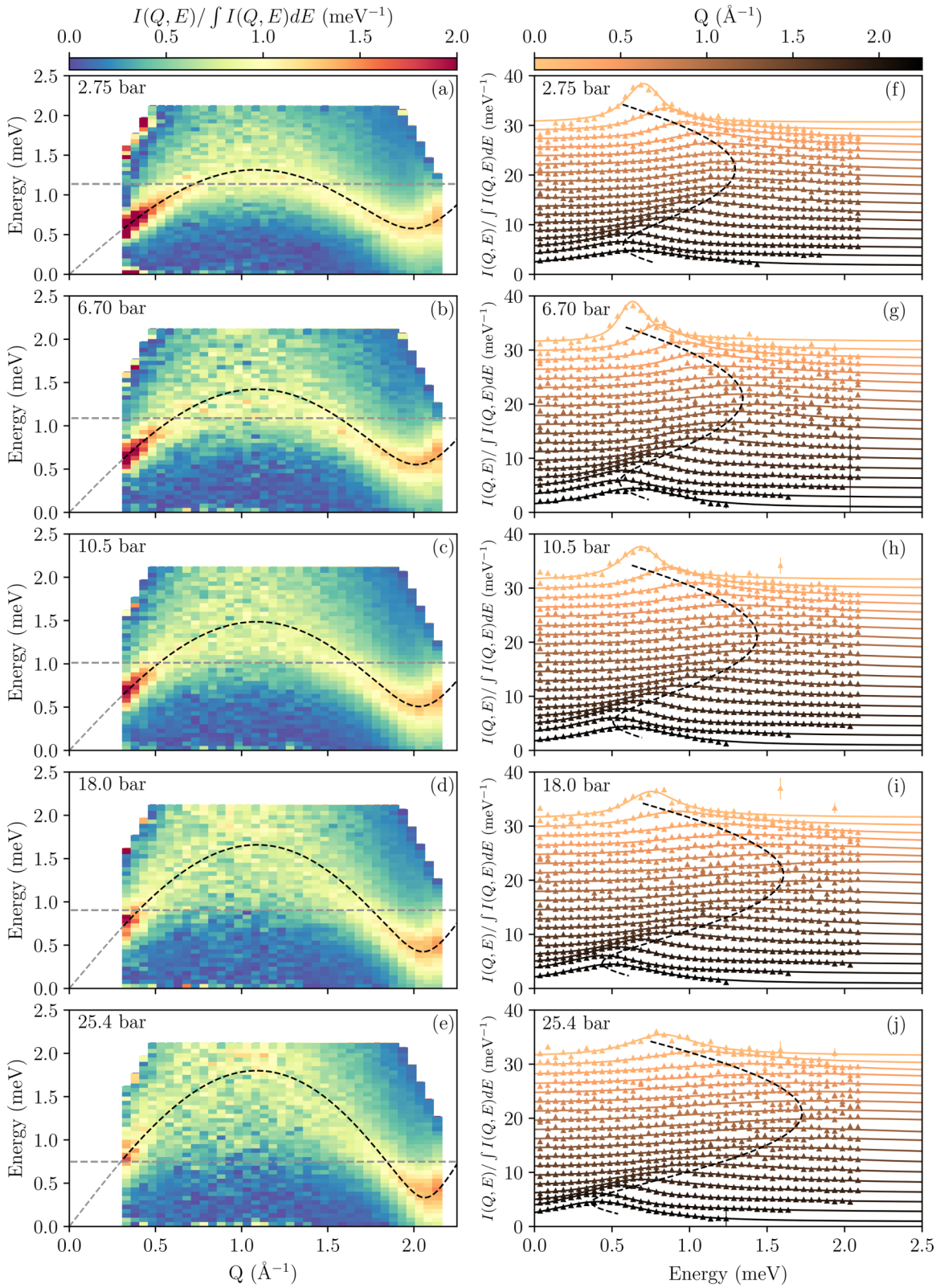

FIG. 3. Breakdown of a phonon-roton sound-wave quasiparticle near the crystallization and superfluid transition. [(a)–(e)] Color contour maps of the spectral density of the measured neutron scattering intensity at pressures $P = 2.75(3)$, 6.76(8), 10.50(3), 18.03(3), and 25.36(3) bars (top to bottom), at temperatures in the 1.7–1.9 K range, as shown in Fig. 1. As in Fig. 2, the dashed curve is the fitted Bogolyubov dispersion without accounting for multiparticle interactions, and the horizontal dashed line marks the decay threshold energy 2Δ. [(f)–(j)] Selected constant-Q cuts of the corresponding spectral density of the measured neutron intensity with fits to the resolution-corrected DHO line shape. The substantial DHO width reflects a short quasiparticle lifetime, which decreases markedly above the decay threshold where the spectral density gets extremely blurred.

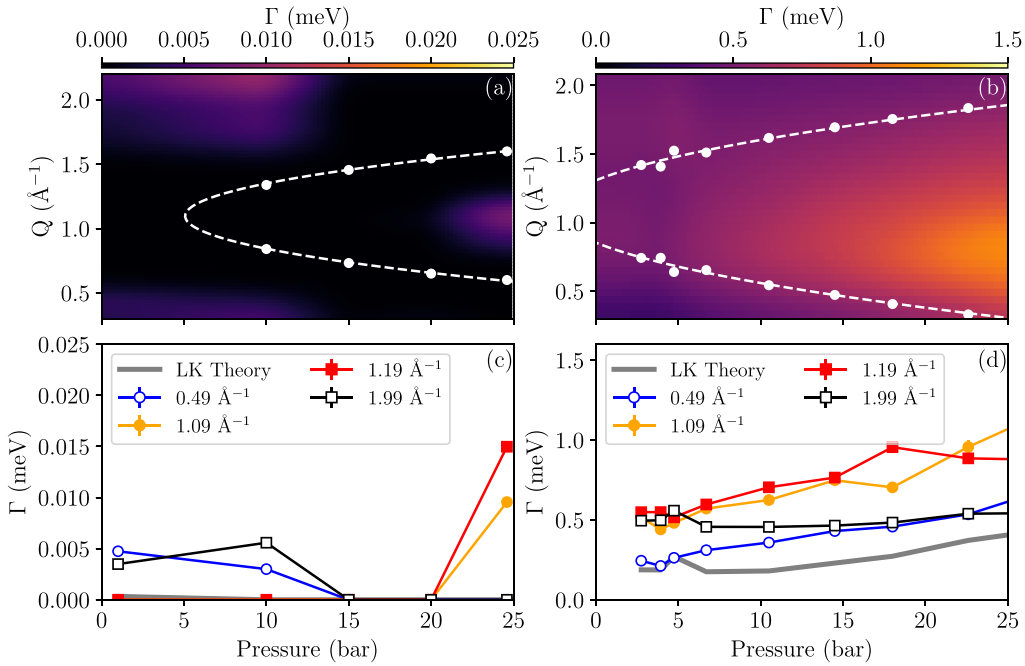

FIG. 4. The quasiparticle width and the breakdown region. Color contour map of the DHO half width at half maximum (HWHM), Γ, which parametrizes the quasiparticle lifetime, $\tau \sim h/\Gamma$, obtained by interpolation of the fit results as a function of pressure, (a) for the low-temperature data of Fig. 2 and (c) for the data of Fig. 3 with pronounced decays. The solid symbols with the parabolic fit (dashed line) show the boundary of the pressure-dependent quasiparticle breakdown region of momenta, $[Q_{c1}, Q_{c2}]$, where decays are allowed for noninteracting quasiparticles with the fitted Bogolyubov dispersion [32–37] of Figs. 2 and 3 (see also Figs. S1– S7 [23]). The pressure dependence of Γ for typical wave vectors in the phonon (open circles), maxon (solid circles and squares), and roton (open squares) regions (c) for the data in (a) and (d) for the data in (b). The gray line shows Γ obtained from LK theory [25,26]. The experimental Γ obtained using a single-component DHO fit is somewhat overestimated by the inclusion of multiparticle states in the fitted intensity, however, its variation with pressure and Q adequately exposes the physics of quasiaprticle decays (see also Supplemental Material [23]). Error bars in all figures show one standard deviation and where not visible are smaller than the symbol size.

Here, we report the experimental observation of an instability towards pair decays leading to the breakdown of a phonon-roton sound wave, an important aspect of quasiparticle behavior in superfluid helium that has been predicted a long time ago. Our present results provide a much-needed completion for the standard model of quantum condensed matter, uncovering the origin of the remaining discrepancies between theory and experiment and unveiling an unusual route to zero-temperature crystallization, which resolves a long-standing puzzle.

We gratefully acknowledge the invaluable technical assistance from J. Leao and NCNR staff. I.Z. is indebted to the late Larry Passell for sharing his wisdom and providing critical advice concerning the INS measurements of liquid helium. We are also grateful to W. Montfrooij, A. Shytov, M. Zhitomirsky, A. Tkachenko, and A. Abanov for valuable discussions. This work at Brookhaven National Laboratory was supported by Office of Basic Energy Sciences (BES), Division of Materials Sciences and Engineering, U.S. Department of Energy (DOE), under Contract No. DE-SC0012704.

[1] P. Kapitza, Nature (London) **141**, 74 (1938).
[2] L. Landau, J. Phys. (USSR) **5**, 71 (1941).
[3] L. Landau, Phys. Rev. **60**, 356 (1941).
[4] L. Landau, J. Phys. (USSR) **11**, 91 (1947).
[5] L. D. Landau, *Collected Papers of L. D. Landau*, edited by D. ter Haar (Elsevier Science, Burlington, MA, 1965), p. 856.
[6] I. M. Khalatnikov, *An Introduction to the Theory of Superfluidity*, Advanced Book Program (Perseus, New York, 2000), p. 206.
[7] D. G. Henshaw and A. D. B. Woods, Phys. Rev. **121**, 1266 (1961).
[8] A. D. B. Woods and R. A. Cowley, Rep. Prog. Phys. **36**, 1135 (1973).
[9] O. W. Dietrich, E. H. Graf, C. H. Huang, and L. Passell, Phys. Rev. A **5**, 1377 (1972).
[10] E. H. Graf, V. J. Minkiewicz, H. B. Møller, and L. Passell, Phys. Rev. A **10**, 1748 (1974).
[11] A. D. B. Woods, P. A. Hilton, R. Scherm, and W. G. Stirling, J. Phys. C: Solid State Phys. **10**, L45 (1977).
[12] W. G. Stirling and H. R. Glyde, Phys. Rev. B **41**, 4224 (1990).

[13] K. H. Andersen, W. G. Stirling, R. Scherm, A. Stunault, B. Fak, H. Godfrin, and A. J. Dianoux, J. Phys.: Condens. Matter **6**, 821 (1994).
[14] B. Fök, L. P. Regnault, and J. Bossy, J. Low Temp. Phys. **89**, 345 (1992).
[15] B. Fåk and J. Bossy, J. Low Temp. Phys. **112**, 1 (1998).
[16] W. Montfrooij, E. C. Svensson, I. M. de Schepper, and E. G. D. Cohen, J. Low Temp. Phys. **109**, 577 (1997).
[17] M. R. Gibbs, K. H. Andersen, W. G. Stirling, and H. Schober, J. Phys.: Condens. Matter **11**, 603 (1999).
[18] W. Montfrooij, E. Svensson, R. Verberg, R. Crevecoeur, and I. de Schepper, arXiv:cond-mat/0603523; W. Montfrooij and E. C. Svensson, J. Low Temp. Phys. **121**, 293 (2000).
[19] K. Beauvois, J. Dawidowski, B. Fåk, H. Godfrin, E. Krotscheck, J. Ollivier, and A. Sultan, Phys. Rev. B **97**, 184520 (2018).
[20] H. Godfrin, K. Beauvois, A. Sultan, E. Krotscheck, J. Dawidowski, B. Fåk, and J. Ollivier, Phys. Rev. B **103**, 104516 (2021).
[21] H. R. Glyde, Rep. Prog. Phys. **81**, 014501 (2018).
[22] K. Beauvois, C. E. Campbell, J. Dawidowski, B. Fåk, H. Godfrin, E. Krotscheck, H.-J. Lauter, T. Lichtenegger, J. Ollivier, and A. Sultan, Phys. Rev. B **94**, 024504 (2016).
[23] See Supplemental Material at http://link.aps.org/supplemental/10.1103/PhysRevB.109.L060502 for additional data presentations, and details of the analysis and fitting.
[24] E. F. Talbot, H. R. Glyde, W. G. Stirling, and E. C. Svensson, Phys. Rev. B **38**, 11229 (1988).
[25] K. H. Andersen, J. Bossy, J. C. Cook, O. G. Randl, and J.-L. Ragazzoni, Phys. Rev. Lett. **77**, 4043 (1996).
[26] B. Fåk, T. Keller, M. E. Zhitomirsky, and A. L. Chernyshev, Phys. Rev. Lett. **109**, 155305 (2012).
[27] L. P. Pitaevskii, Sov. Phys. JETP **9**, 830 (1959).
[28] E. M. Lifshitz and L. P. Pitaevskii, *Statistical Physics, Part 2*, Course of Theoretical Physics Vol. 9 (Butterworth-Heinemann, Oxford, UK, 1980), p. 387.
[29] H. R. Glyde, M. R. Gibbs, W. G. Stirling, and M. A. Adams, Europhys. Lett. **43**, 422 (1998).
[30] M. B. Stone, I. A. Zaliznyak, T. Hong, C. L. Broholm, and D. H. Reich, Nature (London) **440**, 187 (2006).
[31] M. E. Zhitomirsky and A. L. Chernyshev, Rev. Mod. Phys. **85**, 219 (2013).
[32] R. P. Feynman, Phys. Rev. **94**, 262 (1954).
[33] N. N. Bogolyubov and D. N. Zubarev, Sov. Phys. JETP **1**, 83 (1955).
[34] D. Bohm and B. Salt, Rev. Mod. Phys. **39**, 894 (1967).
[35] S. Sunakawa, S. Yamasaki, and T. Kebukawa, Prog. Theor. Phys. **41**, 919 (1969).
[36] A. Isihara and T. Samulski, Phys. Rev. B **16**, 1969 (1977).
[37] I. A. Zaliznyak and J. M. Tranquada, in *Strongly Correlated Systems: Experimental Techniques*, edited by A. Avella and F. Mancini, Springer Series in Solid-State Sciences Vol. 180 (Springer, Berlin, 2014), pp. 205–235.
[38] I. A. Zaliznyak, L.-P. Regnault, and D. Petitgrand, Phys. Rev. B **50**, 15824 (1994).